Strong-field Rydberg-state excitation of nitrogen dioxide pre-excited in the $\tilde{A}^2B_2$ state

Yang Liu, Qi Chen, Tian Sun, Hang Lv,* and Haifeng Xu†
Institute of Atomic and Molecular Physics, Jilin University, Changchun 130012, China

(Received 26 April 2024; accepted 10 June 2024; published 1 July 2024)

We experimentally investigate the Rydberg-state excitation (RSE) process induced by a strong near-infrared (NIR) laser field for nitrogen dioxide (NO_2) molecules which are initially excited in the $\tilde{A}^2B_2$ state by a UV laser field. Both the neutral parent NO_2 and the fragments are observed to survive the strong laser field in high Rydberg states. It is found that the RSE yield of NO_2 ($\tilde{A}^2B_2$) molecules depends on the intensity of the strong NIR laser, as well as the relative polarization and delay time between the NIR and the UV laser fields. Distinct different behaviors between RSE and strong-field ionization of NO_2 ($\tilde{A}^2B_2$) are observed. Analysis indicates that the probability of recapturing the tunneling electron to form high Rydberg states is affected by the molecular orbitals of the excited state, and the RSE process can qualitatively reflect the changes of molecular structure during ultrafast dynamics of the excited state of molecules.

DOI: 10.1103/PhysRevA.110.013101

I. INTRODUCTION

Tunneling ionization of an electron bound to an atom or a molecule acts as the initial step for many physical processes induced by a strong laser field with intensity larger than 10^{13} W/cm^2. After tunneling out, it is possible for the electron to be driven back to and recollide with the ionic core, resulting in various highly nonlinear physical phenomena, including high-order above threshold ionization, nonsequential double ionization, and high-order harmonic generation (HHG) (for reviews, see, e.g., Refs. [1–5]). In addition to these recollision-induced strong-field processes, it is interesting to find that both theoretically and experimentally, tunneling electrons may also be recaptured by ionic Coulomb potential to the Rydberg states, resulting in highly excited neutral atoms [6,7]. Such a Rydberg-state excitation (RSE) process in a strong laser field, also known as frustrated tunneling ionization [7], provides an important complementary aspect to interaction of strong laser fields with atoms or molecules and could be potentially applied for acceleration of neutral particles [8,9] and generation of ultrafast coherent EUV light [10–13]. Thus, it has been the subject of numerous experimental and theoretical studies over the past decade, the majority of which are focused on the strong-field RSE of atoms, with particular interest in the recapture probabilities under different laser fields, the underlying physical mechanism, and the possible quantum effects involved in the process [14–23].

On the other hand, our understanding of the molecular RSE induced by a strong laser fields is still quite limited. Several studies have shown that highly excited neutral atomic fragments can be produced in a strong laser field, which are related to dissociative ionization or Coulomb explosion of some diatomic molecules (e.g., H_2/D_2, N_2, CO, O_2), i.e., neutralization of the corresponding atomic fragment ions by recapturing the tunneled electrons into the highly excited states [24–31]. It is indicated that for an asymmetric molecule such as CO, the probabilities of electrons captured by different atomic fragment ions (C^+ and O^+) to form highly excited atoms (C* and O*) are different, owing to the effect of the molecular orientation and the electronic orbital structure [29]. A joint experimental and theoretical study has demonstrated that neutral diatomic molecules (N_2 and O_2) can survive in highly excited Rydberg states in strong 800-nm laser fields [32]. The behaviors of different molecules are significantly different from those of the corresponding company atoms (Ar and Xe) with ionization potentials I_P similar to those of the molecules (N_2 and O_2), which can be understood by the different structures of molecular orbitals in the recapture picture [32]. Recent theoretical studies using the time-dependent Schrödinger equation and the quantum model have also shown the effect of symmetries of the initial electronic states in the molecular RSE process in strong laser fields [33,34]. The results indicate the excitation probabilities of Rydberg states of molecules with similar ionization potentials but different orbital symmetries are different due to the two-center interference effect and the coherent capture mechanism.

Here, we perform an experimental study on the strong-field RSE process of molecules initially populated in an electronic excited state. Nitrogen dioxide in the first excited state $\tilde{A}^2B_2$ [NO_2 ($\tilde{A}^2B_2$)] is chosen as the target, since it is a simple triatomic molecule but is viewed as a benchmark for study of unimolecular reaction dynamics. Ultrafast time-resolved measurements have been carried out to reveal the underlying physics of the complicated dynamics of NO_2 ($\tilde{A}^2B_2$), using different methods as the probe including ionization [35], electron image [36], channel-resolved ATI [37], HHG [38], and coincidence measurement [39]. Theoretically, in addition to high-level *ab initio* calculations on the structure and potential

*Contact author: lvhang0811@jlu.edu.cn
†Contact author: xuhf@jlu.edu.cn

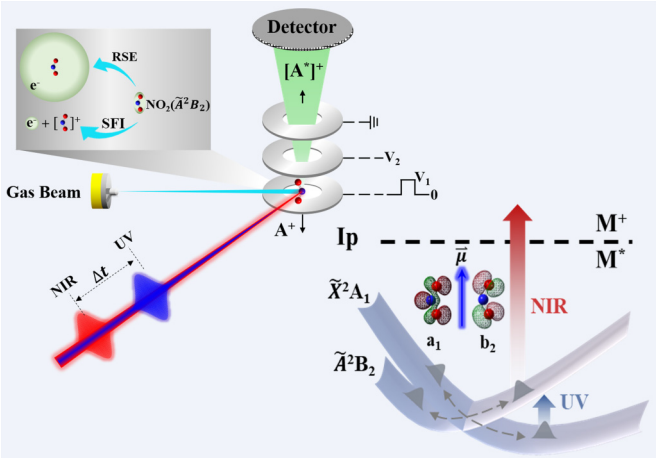

FIG. 1. Schematic illustration of the experimental setup of the tr-PFI-TOF-MS for the investigation of strong-field RSE of NO_2 ($\tilde{A}^2B_2$).

energy surface of the excited states [40,41], time-dependent quantum or semiclassical calculations have been performed on the wave-packet dynamics of NO_2 ($\tilde{A}^2B_2$) [42–45]. While the understanding of the ultrafast dynamics is still far from complete, the overall picture of the evolution in NO_2 ($\tilde{A}^2B_2$) has been established. It is now generally known that after being excited to the $\tilde{A}^2B_2$ state and multiple passage towards the conical intersection along the bending coordinate, the molecules would transfer to the high-vibrational states of $\tilde{X}^2A_1$, followed by intramolecular vibration energy redistribution (IVR) within several hundred femtoseconds, and finally dissociate along the asymmetric stretching mode on a picosecond timescale.

In our study, using the time-resolved pulsed-field-ionization time-of-flight mass-spectrometer (tr-PFI-TOF-MS) method, we experimentally demonstrate that excited molecules can also survive strong laser fields in highly Rydberg states. Both highly excited neutral parents (NO_2*) and fragments (NO*, O*, and N*) are observed in a strong 800-nm laser field after the NO_2 molecules are excited to the $\tilde{A}^2B_2$ state by a weak 400-nm laser field. The RSE yields of NO_2 ($\tilde{A}^2B_2$) are measured as a function of the 800-nm laser intensity as well as the delay time between the two laser pulses, and the results are compared with those of the molecules in the ground state $\tilde{X}^2A_1$. Analysis indicates that the molecular structure and the dynamics in the excited state play a role in the recapture process of molecules in the tunneling ionization region.

The paper is organized as follows. We present our experimental setup of the tr-PFI-TOF-MS in Sec. II. In Sec. III we present our experimental results and a discussion on the mechanism of strong-field RSE of NO_2 ($\tilde{A}^2B_2$). A brief conclusion is given in Sec. IV.

II. EXPERIMENTAL SETUP

The experimental setup of the tr-PFI-TOF-MS is schematically illustrated in Fig. 1. Briefly, the NO_2 molecules are excited to the $\tilde{A}^2B_2$ state from the ground state $\tilde{X}^2A_1$ by a 400-nm laser field. After a delay time, a strong 800-nm laser field is employed to induce strong-field ionization (SFI) or RSE. Highly excited Rydbergs of neutral molecules and fragments from strong-field RSE are measured using a TOF MS operated under a PFI mode. For detection of ions from SFI, a normal TOF-MS is used. For comparison, RSE or SFI of the molecules in the ground state $\tilde{X}^2A_1$ is also investigated by using only the 800-nm laser field.

NO_2 molecules are introduced into the reaction chamber through a 10-μm leak value with a stagnation pressure at 1 atm. The background pressure without gas injection is less than 1×10^{-6} Pa and the working pressure is around 1×10^{-4} Pa in the reaction chamber. The laser system used in the study is a Ti:sapphire femtosecond laser with a central wavelength of 800 nm, a pulse width of ∼50 fs, and a repetition rate of 1 kHz. The output of the laser system is split into two laser beams using a beam splitter. One is frequency doubled by a β-barium borate crystal to produce the second harmonic generation, centered at 400 nm, which is used as the pump pulse to excite the molecules to the $\tilde{A}^2B_2$ state. The other centered at 800 nm is used to induce RSE or SFI. The delay time between the two laser pulses is precisely adjusted by a motor-controlled delay stage. Both the laser beams are recombined by a dichroic mirror, before they are focused by an $f = 25$ cm concave mirror into the interaction region. The pump laser is set to be linearly polarized with the direction parallel to the TOF axis, and the polarization direction of the strong 800-nm laser pulse is adjusted by a half-wave plate. The laser intensity is continuously adjusted by a half-wave plate and a Glan prism.

In our experiments, we utilize a TOF-MS operated under a pulsed electric field to detect highly excited molecules and fragments, as described in detail in our previous studies [31,32]. Any direct ionized ions (M^+, $M = NO_2$, NO, O, or N) after molecules irradiated by the strong field are pushed away from the detector by a dc electric field. After a delay time (τ) of 0.5 μs, the remaining highly excited neutrals (M*) are then field-ionized by switching the voltage of the repulsive plate, and the resulting ions $(M^*)^+$ are detected by microchannel plates at the end of the flight of about 40 cm. In our study, the Rydberg states with principal numbers $20 < n < 30$ are detected, estimated by a saddle-point model of static field ionization [$F = 1/(9n^4)$, F is the electric field]. In the case for detection of direction M^+, standard dc electric fields are applied in the TOF MS, with the voltages kept the same as those in detecting $(M^*)^+$ to ensure identical detection efficiencies.

III. RESULTS AND DISCUSSION

In our tr-PFI-TOF-MS study, the NO_2 molecules are pre-excited to the $\tilde{A}^2B_2$ state from the ground state $\tilde{X}^2A_1$ by a weak UV femtosecond laser field ($\lambda = 400$ nm), followed by strong-field ionization or excitation driven by a NIR laser field ($\lambda = 800$ nm) at a delay time Δt. By measuring the ionic yields as a function of NIR laser intensity (I_{NIR}) and the delay time Δt, we focus on the strong-field RSE of the NO_2 molecules pre-excited in the $\tilde{A}^2B_2$ state. We first show in Fig. 2(a) typical mass spectra after the molecules are irradiated by linearly polarized UV and NIR laser fields with

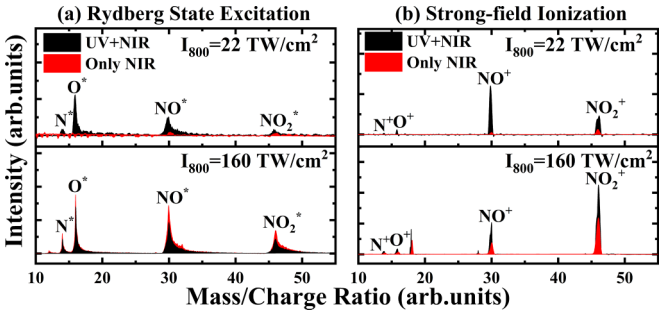

FIG. 2. Typical time-of-flight mass spectra of NO_2 by the linearly polarized UV and NIR laser fields (black) with $\Delta t = 0$ and the polarizations parallel to each other for RSE (a) and SFI (b). The results with only the NIR laser field (red) are presented for comparison.

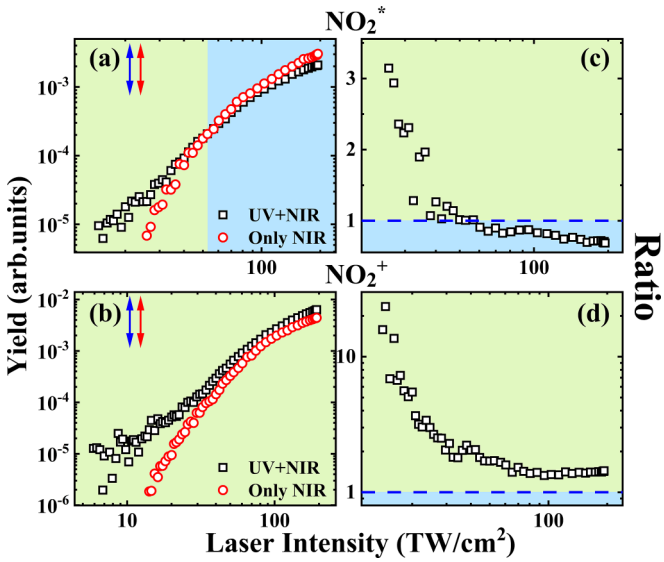

FIG. 3. The yields of (a) NO_2* and (b) NO_2^+ as a function of I_{NIR}, with or without the weak UV pre-excitation laser field. The intensity-dependent ratios R in the UV + NIR laser fields to those in only the NIR laser field for (c) RSE and (d) SFI. The delay time between the UV and NIR laser fields is $\Delta t = 0$ and the laser polarizations are parallel to each other.

$\Delta t = 0$ and their polarizations parallel to each other. The results with only the NIR laser field are also presented in the figure for comparison. Both neutral parent (NO_2*) and fragments (NO*, O*, N*) in high Rydberg states, which are produced by the strong NIR laser field, are observed in the PFI-TOF-MS experiments. Our study provides obvious experimental evidence that NO_2 molecules pre-excited in the $\tilde{A}^2B_2$ state can survive the strong NIR laser field in high Rydberg states. It can be seen that apparent enhancement of the RSE yields is observed in the UV + NIR results comparing to those using only the NIR laser field with I_{NIR} of 22 TW/cm^2 [see the upper panel of Fig. 2(a)]. Interestingly, with increasing I_{NIR} to 160 TW/cm^2, the RSE yields are suppressed in the UV + NIR case [see the lower panel of Fig. 2(a)]. This observation in strong-field RSE is distinctly different from the SFI, in which the yields induced by both laser fields are always higher than those by only the NIR laser field for I_{NIR} at either 22 or 160 TW/cm^2 [see Fig. 2(b)].

To clarify this finding in the strong-field RSE of NO_2 ($\tilde{A}^2B_2$), we further investigate the dependence of the RSE yields on the intensity of the driving NIR laser field. In Fig. 3(a) we show the yields of NO_2* as a function of I_{NIR}, with or without the UV laser field. The results of SFI are presented in Fig. 3(b) for comparison. Both the RSE and SFI yields increase and gradually tend to become saturated with increasing I_{NIR}. However, closer inspection shows that compared to the results in only the NIR laser field, the RSE yields in the UV + NIR case are enhanced at low NIR laser intensity but turn to be suppressed as I_{NIR} is higher than 50 TW/cm^2; while the SFI yields induced by two laser fields are always larger in the whole I_{NIR} range of 15 to 200 TW/cm^2 investigated in the study.

Because of the limited excitation fraction (that is, the NO_2 molecules cannot be completely excited to the $\tilde{A}^2B_2$ state upon absorption of a UV photon), the unexcited molecules would also contribute to the measured RSE (and SFI as well) signals in the UV + NIR experiments, especially for high NIR laser intensity. In order to reveal the strong-field physics of NO_2 molecules initially populated in the $\tilde{A}^2B_2$ state, in the following we evaluate the ratio of the UV + NIR results to those in only the NIR laser field, R, which can be represented as

$$R = \frac{Y_{(\mathrm{UV+NIR})}}{Y_{\mathrm{NIR}}} = \frac{P_A\sigma N_0(X) + P_X(1-\sigma)N_0(X)}{P_X N_0(X)} = \left(\frac{P_A}{P_X} - 1\right)\sigma + 1,$$

where N_0 is the total number of the molecules in the interaction region, σ represents the excitation fraction by the UV photon, P_A and P_X represent the RSE or SFI probabilities of the excited molecules in the $\tilde{A}^2B_2$ state and the unexcited molecules in the ground $\tilde{X}^2A_1$ state, respectively. We assume σ is a constant since the UV laser intensity is fixed during the experiments, and thus the R value will represent the relative probability of the strong-field RSE (or SFI) of NO_2 ($\tilde{A}^2B_2$).

The resulting R values vs I_{NIR} are shown in Figs. 3(c) and 3(d) for RSE and SFI, respectively. It can be seen that, in general, the ratio R for either RSE or SFI decreases upon increasing I_{NIR}, indicating the probability of the excited molecules P_A shows a dependence on the driving laser intensity that is weaker than that of the unexcited molecules P_X. This could be easily understood since the ionization from the excited $\tilde{A}^2B_2$ state tends to become saturated at much lower laser intensity compared to that from the ground $\tilde{X}^2A_1$ state [see Fig. 3(b)], due to the 3.1-eV lower ionization potential (I_P) of the $\tilde{A}^2B_2$ state. Distinct different behaviors of the ratio R for RSE compared with that for SFI are observed in the high driving laser intensity region: for RSE the ratio $R < 1$, indicating $P_A < P_X$ when $I_{NIR} > 50$ TW/cm^2; while for SFI, the ratio R is always larger than 1, indicating $P_A > P_X$ in the whole intensity range investigated in the study [see Figs. 3(c) and 3(d), regions marked with different colors]. It is noted that, for $I_{NIR} > 50$ TW/cm^2, the Keldysh nonadiabatic parameter $\gamma < 1.0$ ($\gamma = \sqrt{\frac{2I_P}{U_P}}$, where I_P and U_P represent the field-free

ionization potential (in eV) and the ponderomotive energy, respectively) [46], indicating tunneling ionization would play a dominant role in the strong-field ionization of the NO_2 molecule. Our results strongly indicate that, in the tunneling ionization region, the RSE probability of the NO_2 molecules initially populated in the $\tilde{A}^2B_2$ state is suppressed comparing to that for the unexcited molecules in the ground $\tilde{X}^2A_1$ state when the polarizations of UV and NIR are parallel to each other.

In the tunneling ionization region, strong-field RSE is described as a recapture process; that is, the photoelectron that first tunnels out through the barrier formed by the Coulomb potential and the external laser field is recaptured by the Coulomb potential in the way it goes out [7,20,32]. The different behaviors between the intensity-dependent R values for RSE and SFI strongly indicate that the suppression in the RSE yields of $NO_2(\tilde{A}^2B_2)$ is attributed to the reduction of the recapture probability rather than the tunneling ionization probability, which would be due to the effect of the structure of the molecular orbitals. In our study, upon absorbing a UV photon to resonantly excite to the $\tilde{A}^2B_2$ state, the NO_2 molecule would be initially aligned along the O-O axis and parallel to the polarization of the pre-excited laser, since the direction of the transition dipole moment for $\tilde{A}^2B_2 \leftarrow \tilde{X}^2A_1$ is parallel to the O-O axis [38,47] (see Fig. 1). Ionization of the NO_2 molecules at the $\tilde{A}^2B_2$ state with the main configuration of $(\cdots)(b_2)^1(a_1)^2$ is dominated by removing an electron in the a_1 orbital, and the electron prefers to emit at the direction perpendicular to the O-O axis [38]. Thus, when the prealigned NO_2 $(\tilde{A}^2B_2)$ molecules are ionized by the strong driving NIR laser with polarization parallel to that of the UV laser (the case used in the experiments in Figs. 2 and 3), the electron would be emitted mainly at the direction that significantly deviates from the field direction of the NIR laser. Therefore, the wave packet of the freed electron would be diffusive, leading to reduced probability to be recaptured in high Rydberg states which locate relatively far away from the ionic core. This finding is in analogous to a previous study on RSE of diatomic molecules (N_2 and O_2), the results of which show remarkably different behaviors in comparison with their companion atoms (Ar and Xe), because of the different capture probabilities which are attributed to their different highest occupied molecular orbitals ($3\sigma_g$ for N_2 and $1\pi_g$ for O_2, respectively) [32].

According to the above discussions, one may expect less suppression of RSE of $NO_2(\tilde{A}^2B_2)$ if we change the field direction of the strong NIR laser to be perpendicular to that of the UV laser. Indeed, as shown in Fig. 4, the RSE yields in the UV + NIR case are larger than those in only the NIR laser field and the ratio $R > 1$ in the I_{NIR} range investigated in the study, the results which are now similar to those of SFI. In the perpendicular setup of the UV + NIR laser fields, the freed electron from the a_1 orbital of NO_2 $(\tilde{A}^2B_2)$ would be mainly distributed along the field direction of the driving NIR laser, and thus the diffusion of electron wave packets would be less significant and less suppression in the recapture probability would be observed comparing to the results in the parallel setup. Therefore, the measured R vs I_{NIR} for RSE presents a tendency similar to that for SFI, as shown in Fig. 4.

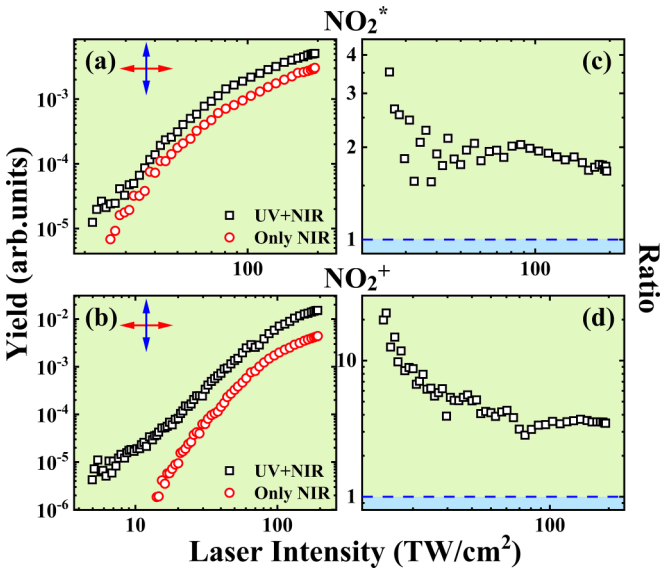

FIG. 4. The yields of (a) NO_2* and (b) NO_2^+ as a function of I_{NIR}, with or without the weak UV pre-excitation laser field. The intensity-dependent ratios R in the UV + NIR laser fields to those in only the NIR laser field for (c) RSE and (d) SFI. The delay time between the UV and NIR laser fields is $\Delta t = 0$ and the laser polarizations are perpendicular to each other.

The above results further confirm the effect of the molecular orbital structure in strong-field RSE of NO_2 $(\tilde{A}^2B_2)$.

In our tr-PFI-TOF-MS study, we can investigate the effect of ultrafast dynamics of the excited state on the strong-field RSE process by measuring the yields as a function of the delay time Δt between the UV and NIR laser pulses. We particularly focus on the RSE of NO_2 $(\tilde{A}^2B_2)$ in high NIR laser intensity $I_{NIR} > 50\,TW/cm^2$ where the molecular orbital effect is more obvious on the recapture probability as we have discussed above. (In the low-I_{NIR} region, since the Rydbergs are mainly produced via multiphoton absorption or Freeman resonance [48–50], the observed intensity-dependent NO_2* is much like that of SFI at either the parallel or the perpendicular case and is not discussed in detail here.) In Fig. 5, we show the ratio R as a function of Δt for both RSE and SFI with the parallel [Fig. 5(a)] or the perpendicular [Fig. 5(b)] setup of the UV + NIR laser fields. Each data point in Fig. 5 is an

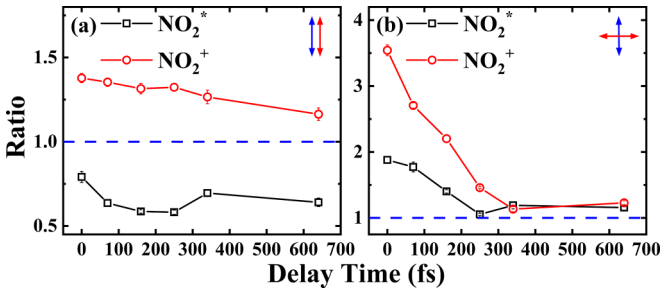

FIG. 5. The time-dependent ratios R in the UV + NIR laser fields to those in only the NIR laser field for NO_2* and NO_2^+. The laser polarizations are (a) parallel or (b) perpendicular to each other and the intensity of the NIR laser fields is 120 TW/cm^2.

averaged result of five measurements at $I_{NIR} = 120\ TW/cm^2$. In general, both yields of RSE and SFI gradually decrease as Δt increases in the range of 0–700 fs. However, in the parallel setup the ratio R of RSE is less than 1, indicating the similar suppressed recapture probability discussed above when the molecule evolves on the surface of $\tilde{A}^2B_2$, while in the perpendicular case the RSE behaves much like the SFI upon varying Δt. It is also worth mentioning that a shoulder is observed at $\Delta t = 340$ fs for RSE which is absent for SFI, indicating the increased recapture probability which could be attributed to the change of the molecular structure induced by the ultrafast dynamics of $\tilde{A}^2B_2$.

The ultrafast dynamics of NO_2 ($\tilde{A}^2B_2$) has been investigated by numerous experimental and theoretical studies reported in the literature [36–38,43,47,51,52]. It is now well known that upon excitation to the $\tilde{A}^2B_2$ state from the ground $\tilde{X}^2A_1$ state, the molecule undergoes multiple passages towards the conical intersection between $\tilde{A}^2B_2$ and $\tilde{X}^2A_1$ along the bending coordinate, followed by transferring to high-vibrational states of $\tilde{X}^2A_1$ via IVR within several hundreds of femtoseconds, and finally could dissociate along the asymmetric stretching coordinate on a picosecond timescale [37,38]. Recent calculations on the wave-packet dynamics of NO_2 ($\tilde{A}^2B_2$) show that the electron wave packet begins to disperse in both $\tilde{X}^2A_1$ and $\tilde{A}^2B_2$ states within ~20 fs [44,45]. Therefore, regardless of RSE or SFI of NO_2 ($\tilde{A}^2B_2$), the probability decreases with the increase of the delay time of the two laser pulses. At $\Delta t \sim 300$ fs, the molecule changes from bending vibration mode to an asymmetrical stretching mode [37]. That is, the molecular structure turns to be linear after ~300 fs, and the electron density of the orbital is mainly along the molecular axis. Thus, the electron released by the NIR laser field prefers to emit along the laser polarization direction. As a result, the probability of being captured to the Rydberg state would be increased, leading to a slight enhancement in the RSE yield at the delay time of ~340 fs as shown in Fig. 5.

We now turn to discuss the fragment RSE of NO_2 ($\tilde{A}^2B_2$) in the tr-PFI-TOF-MS study. Figures 6(a_1) and 6(b_1) show the intensity-dependent R values of NO* and O*, respectively, measured at $\Delta t = 0$ and with the polarizations of the UV and NIR laser fields being parallel or perpendicular to each other. The results of the fragments upon varying Δt at $I_{NIR} = 120\ TW/cm^2$ for both RSE and SFI are shown in Figs. 6(a_2) and 6(b_2) for the parallel setup of the UV + NIR laser fields and in Figs. 6(a_3) and 6(b_3) for the perpendicular case. [The results of the fragment N are not presented because of the poor signal-to-noise ratio]. One can see that either the intensity-dependent or the Δt-dependent yield of each fragment RSE is much like that of the parent RSE. The main findings in the parent RSE as mentioned above [i.e., $R < 1$ in high laser intensity for the parallel setup and R gradually decreases on Δt but shows a slight enhancement at $\Delta t \sim 340$ fs] are also observed in each fragment RSE, indicating that the Rydberg fragments NO* and O* of NO_2 ($\tilde{A}^2B_2$) are directly related to the neutral excited parent NO_2* produced in the strong NIR laser field. Considering the fact that the distribution of the strong-field RSE are dominant with the principal quantum number n around 6–8 [14] and low-lying Rydbergs of polyatomic molecules are usually short-lived [53], we expect

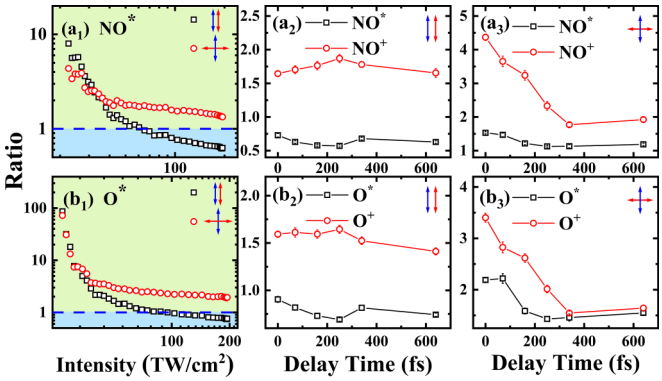

FIG. 6. The intensity-dependent ratios R in the UV + NIR laser fields to those in only the NIR laser field with the laser polarizations are parallel or perpendicular to each other for (a_1) NO* and (b_1) O*. (a_2) and (a_3) The time-dependent ratio R in the UV + NIR laser fields to those in only the NIR laser field for NO* and NO^+. (b_2) and (b_3) The time-dependent ratio R for O* and O^+. The laser polarizations are parallel [panels (a_2) and (b_2)] or perpendicular [panels (a_3) and (b_3)] to each other.

that fragments NO* and O* are formed via the dissociation of the excited neutral molecule NO_2* induced by the recapture process. In addition, the Δt-dependent yield of NO* or O* is apparently different from that of NO^+ or O^+ for the parallel setup [see Figs. 6(a_2) and 6(b_2)], which could be evidence to rule out the mechanism that the excited fragment is produced via the fragment ion capturing a freed electron. Our study indicates that the molecular orbital and the dynamics of NO_2 ($\tilde{A}^2B_2$), which play a role in the recapture probability to produce the highly excited neutral molecule NO_2*, present a similar effect on the formation of the excited fragments NO* and O* in strong NIR laser fields.

IV. CONCLUSIONS

In summary, we present an experimental study on the RSE process of NO_2 ($\tilde{A}^2B_2$) in strong NIR laser fields using the time-resolved pulsed-field-ionization time-of-flight mass-spectrometer method. We find that the neutral NO_2 molecules which are initially populated in the excited state can survive the strong NIR laser fields in high Rydberg states. The laser intensity dependence of the RSE yields of NO_2 ($\tilde{A}^2B_2$) exhibits different behaviors compared to that of strong-field ionization, the results of which depend on the relative polarizations between the NIR and UV laser fields, indicating the effect of molecular orbitals on the electron capture probability. The ultrafast time-resolved measurements on the RSE of NO_2 ($\tilde{A}^2B_2$) are also carried out. Our results indicate that the orbital structure of excited molecular states could affect the capture probability of RSE, and the changes of molecular structure during ultrafast dynamics of excited molecular states could be qualitatively reflected by measuring the strong-field RSE process of excited states.

ACKNOWLEDGMENTS

This work was supported by the National Key Program for S&T Research and Development (Grant No.

2019YFA0307700), the National Natural Science Foundation of China (Grants No. 12174148 and No. 12074144), and the Natural Science Foundation of Jilin Province (Grant No. 20240101322JC).

[1] D. B. Milošević, G. G. Paulus, D. Bauer, and W. Becker, J. Phys. B: At., Mol. Opt. Phys. **39**, R203 (2006).
[2] W. Becker, X. J. Liu, P. J. Ho, and J. H. Eberly, Rev. Mod. Phys. **84**, 1011 (2012).
[3] C. F. de Morisson Faria and X. Liu, J. Mod. Opt. **58**, 1076 (2011).
[4] W. Becker, S. P. Goreslavski, D. B. Milošević, and G. G. Paulus, J. Phys. B: At., Mol. Opt. Phys. **51**, 162002 (2018).
[5] R. A. Ganeev, Laser Phys. Lett. **9**, 175 (2012).
[6] B.-B. Wang, X.-F. Li, P.-M. Fu, J. Chen, and J. Liu, Chin. Phys. Lett. **23**, 2729 (2006).
[7] T. Nubbemeyer, K. Gorling, A. Saenz, U. Eichmann, and W. Sandner, Phys. Rev. Lett. **101**, 233001 (2008).
[8] U. Eichmann, T. Nubbemeyer, H. Rottke, and W. Sandner, Nature (London) **461**, 1261 (2009).
[9] C. Maher-McWilliams, P. Douglas, and P. F. Barker, Nat. Photon. **6**, 386 (2012).
[10] H. Yun, J. H. Mun, Sung In Hwang, S. B. Park, I. A. Ivanov, C. H. Nam, and K. T. Kim, Nat. Photon. **12**, 620 (2018).
[11] M. Matthews, F. Morales, A. Patas, A. Lindinger, J. Gateau, N. Berti, S. Hermelin, J. Kasparian, M. Richter, T. Bredtmann, O. Smirnova, J.-P. Wolf, and M. Ivanov, Nat. Phys. **14**, 695 (2018).
[12] J. H. Mun, I. A. Ivanov, H. Yun, and K. T. Kim, Phys. Rev. A **98**, 063429 (2018).
[13] L. Ortmann, C. Hofmann, I. A. Ivanov, and A. S. Landsman, Phys. Rev. A **103**, 063112 (2021).
[14] H. Zimmermann, J. Buller, S. Eilzer, and U. Eichmann, Phys. Rev. Lett. **114**, 123003 (2015).
[15] S. P. Xu, M. Q. Liu, S. L. Hu, Z. Shu, W. Quan, Z. L. Xiao, Y. Zhou, M. Z. Wei, M. Zhao, R. P. Sun, Y. L. Wang, L. Q. Hua, C. Gong, X. Y. Lai, J. Chen, and X. J. Liu, Phys. Rev. A **102**, 043104 (2020).
[16] F. Sun, C. Lu, Y. Ma, S. Pan, J. Wang, W. Zhang, J. Qiang, F. Chen, H. Ni, H. Li, and J. Wu, Opt. Express **29**, 31240 (2021).
[17] A. S. Landsman, A. N. Pfeiffer, C. Hofmann, M. Smolarski, C. Cirelli, and U. Keller, New J. Phys. **15**, 013001 (2013).
[18] Q. Z. Xia, L. B. Fu, and J. Liu, Phys. Rev. A **87**, 033404 (2013).
[19] H. Zimmermann, S. Patchkovskii, M. Ivanov, and U. Eichmann, Phys. Rev. Lett. **118**, 013003 (2017).
[20] S. Hu, X. Hao, H. Lv, M. Liu, T. Yang, H. Xu, M. Jin, D. Ding, Q. Li, W. Li, W. Becker, and J. Chen, Opt. Express **27**, 31629 (2019).
[21] S. Larimian, S. Erattupuzha, C. Lemell, S. Yoshida, S. Nagele, R. Maurer, A. Baltuška, J. Burgdörfer, M. Kitzler, and X. Xie, Phys. Rev. A **94**, 033401 (2016).
[22] L. Zhao, J. Dong, H. Lv, T. Yang, Y. Lian, M. Jin, H. Xu, D. Ding, S. Hu, and J. Chen, Phys. Rev. A **94**, 053403 (2016).
[23] M. Liu, S. Xu, S. Hu, W. Becker, W. Quan, X. Liu, and J. Chen, Optica **8**, 765 (2021).
[24] A. Emmanouilidou, C. Lazarou, A. Staudte, and U. Eichmann, Phys. Rev. A **85**, 011402(R) (2012).
[25] B. Manschwetus, T. Nubbemeyer, K. Gorling, G. Steinmeyer, U. Eichmann, H. Rottke, and W. Sandner, Phys. Rev. Lett. **102**, 113002 (2009).
[26] J. McKenna, S. Zeng, J. J. Hua, A. M. Sayler, M. Zohrabi, N. G. Johnson, B. Gaire, K. D. Carnes, B. D. Esry, and I. Ben-Itzhak, Phys. Rev. A **84**, 043425 (2011).
[27] W. Zhang, H. Li, X. Gong, P. Lu, Q. Song, Q. Ji, K. Lin, J. Ma, H. Li, F. Sun, J. Qiang, H. Zeng, and J. Wu, Phys. Rev. A **98**, 013419 (2018).
[28] T. Nubbemeyer, U. Eichmann, and W. Sandner, J. Phys. B: At., Mol. Opt. Phys. **42**, 134010 (2009).
[29] W. Zhang, P. Lu, X. Gong, H. Li, Q. Ji, K. Lin, J. Ma, H. Li, F. Sun, J. Qiang, F. Chen, J. Tong, and J. Wu, Phys. Rev. A **101**, 033401 (2020).
[30] J. Wu, A. Vredenborg, B. Ulrich, L. P. H. Schmidt, M. Meckel, S. Voss, H. Sann, H. Kim, T. Jahnke, and R. Dörner, Phys. Rev. Lett. **107**, 043003 (2011).
[31] T. Sun, L. Zhao, Y. Liu, J. Guo, H. Lv, and H. Xu, Phys. Rev. A **108**, 013120 (2023).
[32] H. Lv, W. Zuo, L. Zhao, H. Xu, M. Jin, D. Ding, S. Hu, and J. Chen, Phys. Rev. A **93**, 033415 (2016).
[33] M. Liu, Z. Shu, S. Hu, and J. Chen, J. Phys. B: At., Mol. Opt. Phys. **54**, 095601 (2021).
[34] Z. Shu, M. Liu, S. Hu, and J. Chen, Opt. Express **28**, 11165 (2020).
[35] Y. Liu, T. Sun, L. Zhou, Y. Zhao, Q. Chen, X. Shen, H. Lv, and H. Xu, ChemPhysChem **23**, e202200221 (2022).
[36] D. Irimia, I. D. Petsalakis, G. Theodorakopoulos, and M. H. Janssen, J. Phys. Chem. A **114**, 3157 (2010).
[37] R. Forbes, A. E. Boguslavskiy, I. Wilkinson, J. G. Underwood, and A. Stolow, J. Chem. Phys. **147**, 054305 (2017).
[38] H. J. Wörner, J. B. Bertrand, B. Fabre, J. Higuet, H. Ruf, A. Dubrouil, S. Patchkovskii, M. Spanner, Y. Mairesse, V. Blanchet, E. Mével, E. Constant, P. B. Corkum, and D. M. Villeneuve, Science **334**, 208 (2011).
[39] X. Ding, R. Forbes, M. Kubel, K. F. Lee, M. Spanner, A. Y. Naumov, D. M. Villeneuve, A. Stolow, P. B. Corkum, and A. Staudte, J. Chem. Phys. **151**, 174301 (2019).
[40] V. Kurkal, P. Fleurat-Lessard, and R. Schinke, J. Chem. Phys. **119**, 1489 (2003).
[41] D. Reignier, T. Stoecklin, P. Halvick, A. Voronin, and J. C. Rayez, Phys. Chem. Chem. Phys. **3**, 2726 (2001).
[42] S. Mahapatra, H. Köppel, L. S. Cederbaum, P. Stampfuß, and W. Wenzel, Chem. Phys. **259**, 211 (2000).
[43] A. von Conta, A. Tehlar, A. Schletter, Y. Arasaki, K. Takatsuka, and H. J. Worner, Nat. Commun. **9**, 3162 (2018).
[44] H. Ruf, C. Handschin, A. Ferré, N. Thiré, J. B. Bertrand, L. Bonnet, R. Cireasa, E. Constant, P. B. Corkum, D. Descamps, B. Fabre, P. Larregaray, E. Mével, S. Petit, B. Pons, D. Staedter, H. J. Wörner, D. M. Villeneuve, Y. Mairesse, P. Halvick *et al.*, J. Chem. Phys. **137**, 224303 (2012).
[45] A. Tehlar, A. von Conta, Y. Arasaki, K. Takatsuka, and H. J. Wörner, J. Chem. Phys. **149**, 034307 (2018).

[46] L. V. Keldysh, J. Exptl. Theoret. Phys. (U.S.S.R.) **47**, 1945 (1964) [Sov. Phys. JETP **20**, 1307 (1965)].
[47] P. M. Kraus, Y. Arasaki, J. B. Bertrand, S. Patchkovskii, P. B. Corkum, D. M. Villeneuve, K. Takatsuka, and H. J. Wörner, Phys. Rev. A **85**, 043409 (2012).
[48] E. A. Volkova, A. M. Popov, and O. V. Tikhonova, J. Exp. Theor. Phys. **113**, 394 (2011).
[49] Q. Li, X.-M. Tong, T. Morishita, H. Wei, and C. D. Lin, Phys. Rev. A **89**, 023421 (2014).
[50] R. R. Freeman, P. H. Bucksbaum, H. Milchberg, S. Darack, D. Schumacher, and M. E. Geusic, Phys. Rev. Lett. **59**, 1092 (1987).
[51] B. Liu, J. Zhu, B. Wang, Y. Wang, and L. Wang, J. Phys. Chem. A **113**, 13839 (2009).
[52] M. Sanrey and M. Joyeux, J. Chem. Phys. **125**, 014304 (2006).
[53] M. J. J. Vrakking and Y. T. Lee, J. Chem. Phys. **102**, 8818 (1995).